Spin-to-Charge Conversion in Magnetic Weyl Semimetals

Steven S.-L. Zhang, Anton A. Burkov, Ivar Martin, and Olle G. Heinonen

Spin-to-charge conversion in magnetic Weyl semimetals

Steven S.-L. Zhang[1][*][†], Anton A. Burkov[2], Ivar Martin[1], and Olle G. Heinonen[1,3]

[1]*Materials Science Division, Argonne National Laboratory, Lemont, Illinois 60439, USA*
[2]*Department of Physics and Astronomy, University of Waterloo, Waterloo, Ontario, N2L 3G1, Canada*
[3]*Northwestern-Argonne Institute of Science and Engineering, Evanston, Illinois 60208, USA*
(Dated: August 26, 2019)

Weyl semimetals (WSM) are a newly discovered class of quantum materials which can host a number of exotic bulk transport properties, such as the chiral magnetic effect, negative magnetoresistance, and the anomalous Hall effect. In this work, we investigate theoretically the spin-to-charge conversion in a bilayer consisting of a magnetic WSM and a normal metal (NM), where a charge current can be induced in the WSM by a spin current injection at the interface. We show that the induced charge current exhibits a peculiar anisotropy: it vanishes along the magnetization orientation of the magnetic WSM, regardless of the direction of the injected spin. This anisotropy originates from the unique band structure of magnetic WSMs and distinguishes the spin-to-charge conversion effect in WSM|NM structures from that observed in other systems, such as heterostructures involving heavy metals or topological insulators. The induced charge current depends strongly on injected spin orientation, as well as on the position of the Fermi level relative to the Weyl nodes and the separation between them. These dependencies provide additional means to control and manipulate spin-charge conversion in these topological materials.

Central to spintronics are the inter-conversion between charge and spin currents, and the manipulation and detection of the spin orientation of current-carrying itinerant electrons. Inter-conversion can utilize the spin Hall effect (SHE) [1–5] and the inverse spin Hall effect (ISHE) – the Onsager reciprocal of the SHE that originates in bulk spin-orbit interactions; the SHE and ISHE are well-established phenomena which convert a charge current to a spin current (SHE), and a spin current to a charge current propagating perpendicularly to both the spin and flow directions of the injected spin current (ISHE). The ISHE has been playing an important role in detecting spin current generation in various heterostructures via transport measurements [5, 6].

Recently, several experimental and theoretical studies [7–14] have investigated the inverse Edelstein effect (IEE) in an interfacial two-dimensional electron gas (2DEG) with Rashba spin-splitting, or in a 2DEG at the surface of a three-dimensional (3D) topological insulator. In the IEE a spin accumulation in the 2DEG induces a charge current flowing perpendicularly to the nonequilibrium spin orientation. Compared to the ISHE that typically occurs in bulk systems, the spin-to-charge conversion based on the IEE is arguably more efficient by taking advantage of the remarkable spin-momentum locking arising from strong interfacial spin-orbit coupling as well as of broken inversion symmetry at the interface involving a heavy metal or topological insulator layer.

Weyl semimetals (WSMs), a newly discovered class of quantum materials, is another rapidly evolving research field [15–18]. This novel semimetal possesses distinct electronic properties, such as the chiral anomaly [19–21] and Fermi arc surface states [22], that are protected by the nontrivial topology of the band structure. WSMs studied to date have broken inversion symmetry (but are time-reversal invariant) with at least four, and often many more, Weyl nodes. The relatively large number of Weyl nodes makes it difficult to clearly elucidate and control effects related to the location of the Weyl nodes, and the lack of a magnetic order parameter prevents direct coupling to magnetic fields. Recently, there has been increasing interest in the pursuit of magnetic WSMs, which can have only two Weyl nodes present near the Fermi surface — an ideal system to investigate transport properties — and also allow for direct coupling with external magnetic field to control and manipulate electronic and transport properties. Most efforts have been dedicated to seeking potential candidates of magnetic WSMs [23–26] and examining their bulk transport properties. In contrast, little attention has been paid to the coupled spin and charge degrees of freedom in heterostructures composed of magnetic WSMs and other materials, which is of fundamental interest and may be important for future applications of WSMs in spintronics.

In this work, we investigate theoretically the spin-to-charge conversion in a bilayer consisting of a magnetic WSM with two Weyl nodes and a nonmagnetic metal (NM), as shown schematically in Fig. 1(a). We will show that a charge current can be induced in the magnetic WSM by injecting a spin current from the NM and that unique properties of magnetic WSMs allow for a control

_____

[*]Email: shulei.zhang@case.edu
[†]Present address: Department of Physics, Case Western Reserve University, Cleveland, Ohio 44106, USA
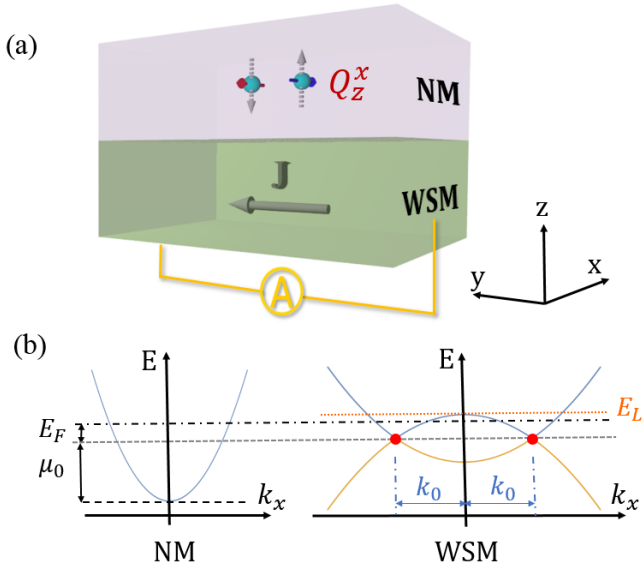
FIG. 1: Schematics of spin-to-charge conversion in a bilayer consisting of a normal metal (NM) and a magnetic Weyl semimetal (WSM). Panel (a): A spin current Q_z^α flowing in the z-direction (perpendicular to the layer plane) and with spin polarized in an arbitrary direction (denoted by the superscript "α") is generated in the NM layer, which is subsequently converted to a charge current $\boldsymbol{J}$ in the WSM layer. Panel (b): sketches of band diagrams $E(\mathbf{k})$ with $k_y = k_z = 0$ for the NM and the WSM with the dash-dotted line and the dash line denoting respectively the Fermi energy E_F and the conduction band bottom of the NM with respect to the energy of the pair of Weyl nodes (red dots) which are separated by $2k_0$; the orange dotted line denotes the Lifshitz transition energy E_L above which two separate Fermi surfaces, enclosing the two Weyl nodes, merge into a single one.

of the spin-to-charge conversion that has no analog in NM|conventional-ferromagnet bilayer systems.

We commence with the following minimal model Hamiltonian [18, 27] for the magnetic WSM layer filling the $z < 0$ half space:

$$\mathcal{H}_W = \left[m_1 \left(k_0^2 - k_x^2 \right) + m_0 \left(k_y^2 + k_z^2 \right) \right] \sigma_x + v \left(k_y \sigma_y + k_z \sigma_z \right), \tag{1}$$

where σ_i ($i = x, y$ and z) are Pauli spin matrices, and m_0, m_1 and v are generic materials parameters. Note that the two Weyl nodes are located at $\mathbf{k} = (\pm k_0, 0, 0)$ and that the first term on the right-hand-side of Eq. (1) breaks time-reversal symmetry. The Weyl Hamiltonian has the eigenvalues

$$E_{\mathbf{k},s} = s \sqrt{\left[m_1 \left(k_0^2 - k_x^2 \right) + m_0 \left(k_y^2 + k_z^2 \right) \right]^2 + v^2 \left(k_y^2 + k_z^2 \right)}, \tag{2}$$

where $s = \pm 1$ with $E_{\mathbf{k},+}$ and $E_{\mathbf{k},-}$ corresponding to the upper and lower energy bands that touch at the pair of Weyl nodes. The $z \geq 0$ region is occupied by a NM described by the Hamiltonian $\mathcal{H}_N = \frac{\hat{p}^2}{2m_e} - \mu_0$, where m_e is the effective mass and μ_0 denotes the deviation of

the conduction band bottom of the NM layer from the energy of the two Weyl nodes, as sketched in Fig. 1(b). Note that we will only consider $\mu_0 > 0$ so that there are available scattering states in the NM when the two Weyl nodes are in the close vicinity of the Fermi energy, which are the circumstances under which most of the interesting transport phenomena in WSMs emerge [28–31].

In the NM, by choosing the z-axis as the spin quantization axis, the full scattering wave function for a free electron with a given energy E and a spin pointing in an arbitrary direction $\boldsymbol{n} = (\sin\theta \cos\phi, \sin\theta \sin\phi, \cos\theta)$ can be written as a linear combination of spin-up and spin-down components, i.e.,

$$\varphi_N(\mathbf{k}, \mathbf{r}) = \left[\cos\frac{\theta}{2} e^{-i\phi/2} \begin{pmatrix} 1 \\ 0 \end{pmatrix} \left(e^{-ik_z z} + R_\uparrow e^{ik_z z} \right) \right.$$
$$\left. + \sin\frac{\theta}{2} e^{i\phi/2} \begin{pmatrix} 0 \\ 1 \end{pmatrix} \left(e^{-ik_z z} + R_\downarrow e^{ik_z z} \right) \right] e^{i\mathbf{k}_\parallel \cdot \mathbf{r}}, \tag{3}$$

where $k_z \equiv \sqrt{\frac{2m_e E}{\hbar^2} - \mathbf{k}_\parallel^2}$ with $\sigma = \uparrow$ ($\downarrow$) and $\mathbf{k}_\parallel [\equiv (k_x, k_y)]$ the in-plane component of the wavevector, R_σ are the reflection amplitudes, and we have assumed translational invariance in the x-y plane.

The wave function for an electron transmitted into the magnetic WSM can be expressed as

$$\varphi_W(\mathbf{k}, \mathbf{r}) = \left(T_+ \chi_+ e^{ik_{z,+} z} + T_- \chi_- e^{ik_{z,-} z} \right) e^{i\mathbf{k}_\parallel \cdot \mathbf{r}}, \tag{4}$$

where $T_\pm$ are the transmission amplitudes, χ_+ and χ_- are two spinors given by $\chi_\pm = \frac{1}{\sqrt{N_\pm}} \begin{pmatrix} a_\pm \\ b_\pm \end{pmatrix}$ with $a_\pm = m_0 \left(\gamma_k + k_{z,\pm}^2 - i k_v k_y \right)$ [where we have defined $k_v \equiv \frac{v}{m_0}$ and $\gamma_k \equiv \frac{m_1}{m_0} \left(k_0^2 - k_x^2 \right) + k_y^2$], $b_\pm = E - v k_{z,\pm}$ and $N_\pm$ the normalization coefficients satisfying $|a_\pm|^2 + |b_\pm|^2 = N_\pm^2$. The z-components of the wavevectors are given by

$$k_{z,\pm}^2 = -\gamma_k - \frac{1}{2} k_v^2 \pm \sqrt{\left(\gamma_k - k_y^2 + \frac{1}{4} k_v^2 \right) k_v^2 + \left(\frac{E}{m_0} \right)^2}. \tag{5}$$

Note that the signs of $k_{z,\pm}$ are so selected that the transmitted waves either propagate freely or decay in the WSM ($z < 0$).

The reflection and transmission amplitudes $R_{\uparrow(\downarrow)}$ and $T_\pm$ can be determined by proper boundary conditions. Here, we assume that both the scattering wave function and the z-component of the current density are continuous at the interface $z = 0$:

$$\varphi_N(0^+) = \varphi_W(0^-) \tag{6a}$$

$$\hat{v}_{N,z} \varphi_N(0^+) = \hat{v}_{W,z} \varphi_W(0^-) \tag{6b}$$

where the velocity operators are given by $\hat{\boldsymbol{v}}_N = \frac{\partial \mathcal{H}_N}{\hbar \partial \mathbf{k}}$ and $\hat{\boldsymbol{v}}_W = \frac{\partial \mathcal{H}_W}{\hbar \partial \mathbf{k}}$ for the NM and WSM, respectively, and we have eliminated a common phase factor of $e^{i\mathbf{k}_\parallel \cdot \mathbf{r}}$.
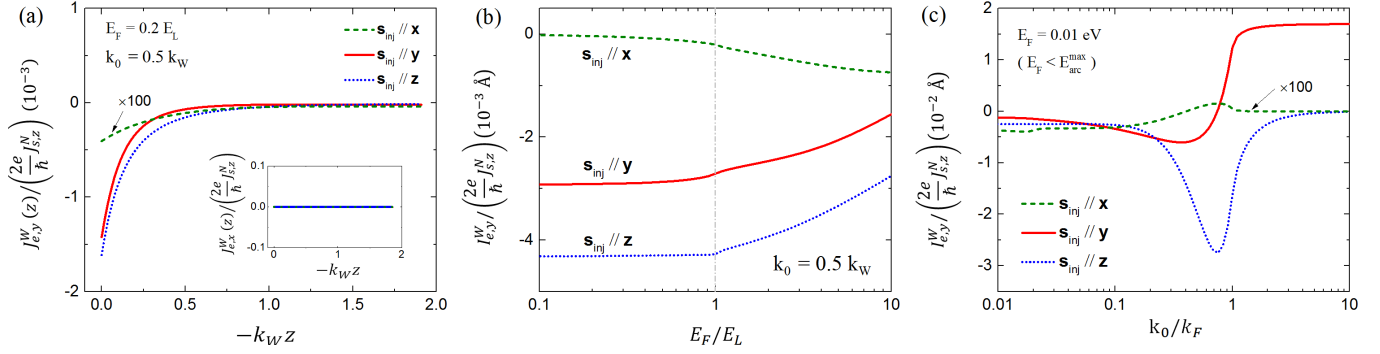
2

FIG. 2: Characterization of the induced charge current in the magnetic WSM layer: (a) Current density $\boldsymbol{J}_{e,\parallel}^W$ as a function of the spatial coordinate z, the spatially integrated current $\boldsymbol{I}_{e,\parallel}^W \left(\equiv \int_{-\infty}^0 dz \boldsymbol{J}_{e,\parallel}^W \right)$ as functions of (b) Fermi energy E_F and (c) the separation of the two Weyl nodes k_0 for an injected spin $\boldsymbol{s}_{inj}$ along x, y and z axes respectively. The Lifshitz transition energy, the maximum energy of the Fermi arc state, and the Fermi wavevector are given by $E_L = m_0 k_0^2$, $E_{arc}^{max} = |v| k_0$ and $k_F = \sqrt{2m_e(E_F + \mu_0)/\hbar^2}$, respectively. We have introduced a wavevector $k_W \equiv v/m_0$ **which only depends on the material parameters of the WSM.** Other parameters used in the numerical calculation: $\mu_0 = 5.0$ eV, $m_e = 9 \times 10^{-31}$ kg, $m_0 = -m_1 = 20$ eV·$\mathring{A}^2$ and $v = 2$ eV·$\mathring{A}$.

Thus far, we have solved the problem of a single electron scattering at the interface of the magnetic-WSM|NM bilayer [32]. To calculate the current density induced in the magnetic WSM layer due to the spin current injection, we need to find the electron distributions in each layer. At the NM side of the interface (i.e., $z = 0^+$), the distribution function can be described by a 2×2 matrix in spin space [33–36], i.e.,

$$\hat{f}_N = f_{0,N}(\mathbf{k})\hat{I} + \hat{g}_N(\mathbf{k}) \tag{7}$$

where $f_{0,N}(\mathbf{k})$ is the equilibrium distribution function, $\hat{I}$ is the 2×2 identity matrix and the nonequilibrium component of the distribution function $\hat{g}_N(\mathbf{k})$ that gives rise to the spin current can be described by

$$\hat{g}_N(\mathbf{k}) = -e\tau v_z \hat{\mathcal{E}}_z \frac{\partial f_0}{\partial E_{\mathbf{k}}} \tag{8}$$

where $\hat{\mathcal{E}}_z (= E_z \boldsymbol{\sigma} \cdot \boldsymbol{s}_{inj}$ with $\boldsymbol{\sigma}$ denoting the Pauli spin matrices and a unit vector $\boldsymbol{s}_{inj}$ denoting the spin direction of the spin current) is a spin-dependent electric field pointing in opposite directions for electrons with opposite spin directions which drives a spin current [48]. At temperatures well below the Fermi temperature of the NM, one can assume $\frac{\partial f_{0,N}}{\partial E_{\mathbf{k}}} \simeq -\delta(E_{\mathbf{k}} - \mu_0 - E_F)$ where E_F is the Fermi energy relative to the energy of the two Weyl nodes. Formally, the spin current density is given by $Q_z^\alpha = \frac{\hbar}{4}Tr_\sigma \int \frac{d^3\mathbf{k}}{(2\pi)^3}\sigma^\alpha v_z \hat{f}_N$. Explicitly, $Q_z^b = J_{s,z}^N s_{inj}^b$ where the magnitude of the spin current density for a given spin direction can be characterized by $J_{s,z}^N \equiv \frac{\hbar}{2e}\sigma_D E_z$ with $\sigma_D = \frac{\tau e^2 k_F^3}{3\pi^2 m_e}$ the Drude conductivity.

The nonequilibrium distribution function for the transmitted electrons in the magnetic WSM is determined by

the transmission amplitudes [32] and the nonequilibrium electron distribution $\hat{g}_N(\mathbf{k})$ at $z = 0^+$ [33, 37] via

$$\hat{g}_W^<(\mathbf{k}, z) = \hat{T}^\dagger(\mathbf{k}, z)\hat{g}_N^<(\mathbf{k})\hat{T}(\mathbf{k}, z) \tag{9}$$

where $\hat{T}(\mathbf{k}, z)$ is a 2×2 transmission matrix satisfying $\varphi_W(\mathbf{k}, z) = \hat{T}(\mathbf{k}, z)\varphi_{N,i}(\mathbf{k}, 0^+)$ with $\varphi_{N,i}$ the incident wave function [32], and the superscript "$<$" denotes electrons moving in the negative z-direction (i.e., $v_z < 0$). Note that, to the leading order, electrons in the WSM moving towards the interface are assumed to entirely come from the equilibrium distribution, i.e., $\hat{f}_W^> \simeq \hat{f}_{0,W}^>$ and $\hat{g}_W^> \simeq 0$.

Having obtained the nonequilibrium distribution $\hat{g}_W$ $(= \hat{g}_W^> + \hat{g}_W^<)$, the in-plane charge current density induced in the magnetic WSM layer can be computed via

$$\boldsymbol{J}_{e,\parallel}^W(z) = -\frac{e}{2}\int \frac{d^3\mathbf{k}}{(2\pi)^3}Tr_\sigma\left(\hat{g}_W \hat{\boldsymbol{v}}_{W,\parallel} + h.c.\right), \tag{10}$$

where $h.c.$ denotes Hermitian conjugate and the trace operation is carried out in the spin space [49].

Before seeking the numerical solutions of the induced charge current in the magnetic WSM layer, a remarkable property of the spin-to-charge conversion can be illuminated by a simple symmetry analysis of Eq. (10): regardless of the orientation of the injected spins, no current will be induced in the direction parallel to the line connecting the pair of Weyl nodes in momentum space, i.e., $J_{e,x}^W = 0$. This is simply because the x-component of the velocity operator $\hat{v}_{W,x}$ is an odd function of k_x whereas the nonequilibrium distribution function $\hat{g}_W$ is an even function of k_x. Therefore, the corresponding x-component of the current density must vanish everywhere in the magnetic WSM layer as it is the integral of the product of these two over $\mathbf{k}$-space. Such an anisotropic

spin-to-charge conversion stems from the inherent property of magnetic WSMs – the anisotropy in the band structure in the first Brillouin zone between the directions perpendicular and parallel to the vector connecting the two Weyl nodes in **k**-space. The numerical solution of $J_{e,x}^W$ indeed confirms that it vanishes everywhere in the magnetic WSM layer, regardless of the direction of the injected spin, the position of the Fermi level as well as the separation between the Weyl nodes [see the inset of Fig. 2(a)].

In contrast to the robust suppression of $J_{e,x}^W$, the behavior of the current induced in the y-direction is much richer. Figure 2(a) shows the spatial variation of the $J_{e,y}^W(z)$ for the injected spin along x, y and z directions, respectively. We find that while the magnitude of $J_{e,y}^W$ depends on the orientation of the spin injection, it generally decays rapidly away from the WSM|NM interface (within 1 nm, given the parameters $m_0 = 20$ eV·$\mathring{A}^2$ and $v = 2$ eV·$\mathring{A}$), indicating a dominant contribution of the evanescent surface states to the spin-to-charge conversion in the magnetic WSM. **We will discuss the physical nature of these evanescent surface states below.**

In Fig. 2(b), we show the total induced current $I_{e,y}^W \left(\equiv \int_{-\infty}^0 dz J_{e,y}^W \right)$ as a function of the Fermi level E_F. We note the existence of a Lifshitz transition energy level E_L at which two separate Fermi surfaces, enclosing the two Weyl nodes, merge into a single Fermi surface [as shown schematically in Fig. 1(b)]. We find that the total current $I_{e,y}^W$ is insensitive to the variation of the Fermi level as long as E_F is below E_L, and the onset of noticeable changes of $I_{e,y}^W$ occur at E_L due to a significant change of density of states at the Fermi level when it crosses the Lifshitz energy.

In Fig. 2(c), we show the dependence of the total induced current $I_{e,y}^W$ on the separation between the two Weyl nodes $2k_0$. **When $k_0 < k_F$, the induced charge current is finite for all three spin injection directions, but when $k_0 > k_F$ significant spin-to-charge conversion only occurs when spin is injected in the y-direction, which indicates that the Fermi arc states with spin locked in the y-direction [38] may play a dominant role in this case.**

We are now in a position to discuss the role of the Fermi arc states plays in the spin-to-charge conversion effect. It can be shown that the Fermi arc surface states are derived by imposing open boundary condition at the interface $z = 0$, i.e., $\varphi_W(0) = 0$ [38]. However, different interfacial boundary conditions [Eqs. (6a) and (6b)] are imposed in the scattering problem that we consider here. Therefore, while the Fermi arc states are constructed from linear combinations of degenerate evanescent solutions so that open boundary condition is satisfied, different linear com- binations of these degenerate evanescent states form admissible solutions that satisfy the interfacial boundary conditions used here [39]. Furthermore, in order for the building blocks of the Fermi arc states to play a dominant role in the spin-charge conversion, there are two necessary conditions : 1) the Fermi level (relative to the Weyl nodes) must be smaller than the maximum energy of the Fermi arc states, i.e., $E_F < E_{arc}^{max}$; 2) the Fermi wavevector of the normal metal k_F is no larger than k_0, i.e, $k_F \leq k_0$ (in this case, admissible evanescent states other than those that make up the Fermi arc states are largely excluded) [39].**

Very recently, a magnetic WSM EuCd$_2$As$_2$ was predicted to contain only a single pair of Weyl nodes [26]. It would be interesting to provide an order-of-magnitude estimation of the effect for this material. Choosing the following parameters for EuCd$_2$As$_2$ [40]: $m_0 = 1.6$ eV·$\mathring{A}^2$, $m_1 = 54.5$ eV·$\mathring{A}^2$, $v = 2.7$ eV·$\mathring{A}$, $k_0 = 0.008$ $\mathring{A}^{-1}$, and $E_F = 0.01$ eV, we obtain a spin-to-charge conversion efficiency of $\vartheta \simeq 0.2\%$ for spin injected along the y-direction where $\vartheta \equiv J_{e,y}^W(0^-)/(\frac{2e}{\hbar} J_{s,z}^N)$, which is **of the same order of magnitude as the spin Hall angle of Au [6, 41].**

As a final point, it is interesting to compare the spin-to-charge conversion in magnetic WSMs with that in other systems. When a spin current is injected in heavy metals (such as Pt or Ta), a charge current will be generated in the direction perpendicular to both the spin and the flow directions of the injected spin current due to the ISHE. A transverse charge current can also be generated, based on the IEE, by injecting a spin current perpendicularly to the surface of a topological insulator or to an interface with strong Rashba spin-orbit coupling and using the spin-momentum locking in these systems that fixes the spins of the carriers perpendicularly to their momenta. For both IEE and ISHE, a charge current may in principle be induced in any arbitrary direction with properly chosen spin injection direction [42]; in this sense these two effects are isotropic. **Another system of potential interest is nodal-line semimetal wherein nonaccidental band-crossing occurs along lines in the Brillouin zone [18, 43, 44]. Spin-to-charge conversion effect may occur in this type of semimetals when there is spin-splitting along the nodal lines due to broken inversion or time reversal symmetry. For an ideal nodal-ring semimetal with band-crossing along a circle in a k_x-k_y plane, we would expect the effect to be isotropic as well due to the rotational symmetry of the energy dispersion about the k_z-axis (provided the flow direction of the injected spin current is perpendicular to the x-y plane).**

The spin-to-charge conversion in magnetic WSMs, however, is rather *anisotropic* emanating from the anisotropy in their unique band structures – the appear-

ance of a pair of Weyl nodes in $\mathbf{k}$-space; as we have shown above, no charge current can be induced in the direction along the line connecting the two Weyl nodes (i.e., $\hat{\mathbf{k}}_0$), regardless of the orientation of the injected spins. Note that for a magnetic WSM with a single pair of Weyl nodes, the magnetization is in the same direction as $\hat{\mathbf{k}}_0$ [40]. In general, there will be an odd number of pairs in a magnetic WSM, in which case the total current density, being the sum of contributions from different pairs (if the pairs of Weyl nodes are well separated in the reciprocal space), vanishes along the magnetization direction, i.e.,

$$\mathbf{m} \cdot \boldsymbol{J}_{e,\parallel}^W = 0 \,, \tag{11}$$

where $\mathbf{m}$ is a unit vector denoting the magnetization direction of the magnetic WSM.

A charge current, however, can be induced in the direction perpendicular to the magnetization direction, and the induced current is rather sensitive to the direction of the injected spin, which is experimentally controllable. In addition, we have shown that the spin-to-charge conversion in magnetic WSMs relies on the separation between two Weyl nodes and the position of the Fermi surface relative to them, which provides additional means to manipulate and control the effect. These remarkable features make the spin-to-charge conversion in magnetic WSMs distinctly different from that previously studied in heterostructures involving heavy metals or topological insulators. **Recently, a large bulk anomalous Hall effect (with anomalous Hall angle of 20%) was observed in the magnetic WSM $Co_3Sn_2S_2$ [45, 46]. It would be of great interests to explore the spin-to-charge conversion in layered structures such as Py|Cu|WSM or YIG|Cu|WSM (with WSM being $Co_3Sn_2S_2$ or $EuCd_2As_2$) wherein a spin current can be injected from the other magnetic layer (Py or YIG) via spin pumping.**

[1] M. Dyakonov and V. Perel, Phys. Lett. A **35**, 459 (1971).
[2] J. E. Hirsch, Phys. Rev. Lett. **83**, 1834 (1999).
[3] S. Zhang, Phys. Rev. Lett. **85**, 393 (2000).
[4] G. Vignale, J. Supercond. Novel Magn. **23**, 3 (2010).
[5] J. Sinova, S. O. Valenzuela, J. Wunderlich, C. H. Back, and T. Jungwirth, Rev. Mod. Phys. **87**, 1213 (2015).
[6] A. Hoffmann, IEEE Trans. Magn. **49**, 5172 (2013).
[7] J. C. R. Sánchez, L. Vila, G. Desfonds, S. Gambarelli, J. P. Attané, J. M. De Teresa, C. Magén, and A. Fert, Nat. Commun. **4**, 2944 (2013).
[8] K. Shen, G. Vignale, and R. Raimondi, Phys. Rev. Lett. **112**, 096601 (2014).
[9] Y. Shiomi, K. Nomura, Y. Kajiwara, K. Eto, M. Novak, K. Segawa, Y. Ando, and E. Saitoh, Phys. Rev. Lett. **113**, 196601 (2014).
[10] E. Lesne, Y. Fu, S. Oyarzun, J. C. Rojas-Sánchez, D. C. Vaz, H. Naganuma, G. Sicoli, J.-P. Attané, M. Jamet, E. Jacquet, J.-M. George, A. Barthélémy, H. Jaffrès, A. Fert, M. Bibes, and L. Vila, Nat. Mater. **15**, 1261 (2016).
[11] J.-C. Rojas-Sánchez, S. Oyarzún, Y. Fu, A. Marty, C. Vergnaud, S. Gambarelli, L. Vila, M. Jamet, Y. Ohtsubo, A. Taleb-Ibrahimi, P. Le Fèvre, F. Bertran, N. Reyren, J.-M. George, and A. Fert, Phys. Rev. Lett. **116**, 096602 (2016).
[12] S. Zhang and A. Fert, Phys. Rev. B **94**, 184423 (2016).
[13] D. Yue, W. Lin, J. Li, X. Jin, and C. L. Chien, Phys. Rev. Lett. **121**, 037201 (2018).
[14] W. Han, Y. Otani, and S. Maekawa, npj Quantum Materials **3**, 27 (2018).
[15] A. A. Burkov, Nat. Mater. **15**, 1145 (2016).
[16] B. Yan and C. Felser, Annu. Rev. Condens. Matter Phys. **8**, 337 (2017).
[17] M. Z. Hasan, S.-Y. Xu, I. Belopolski, and S.-M. Huang, Annu. Rev. Condens. Matter Phys. **8**, 289 (2017).
[18] N. P. Armitage, E. J. Mele, and A. Vishwanath, Rev. Mod. Phys. **90**, 015001 (2018).
[19] S. L. Adler, Phys. Rev. **177**, 2426 (1969).
[20] J. S. Bell and R. Jackiw, Il Nuovo Cimento A (1965-1970) **60**, 47 (1969).
[21] H. Nielsen and M. Ninomiya, Phys. Lett. B **130**, 389 (1983).
[22] X. Wan, A. M. Turner, A. Vishwanath, and S. Y. Savrasov, Phys. Rev. B **83**, 205101 (2011).
[23] Z. Wang, M. G. Vergniory, S. Kushwaha, M. Hirschberger, E. V. Chulkov, A. Ernst, N. P. Ong, R. J. Cava, and B. A. Bernevig, Phys. Rev. Lett. **117**, 236401 (2016).
[24] Kübler, J. and Felser, C., EPL **114**, 47005 (2016).
[25] W. Shi, L. Muechler, K. Manna, Y. Zhang, K. Koepernik, R. Car, J. van den Brink, C. Felser, and Y. Sun, Phys. Rev. B **97**, 060406 (2018).
[26] L.-L. Wang, N. H. Jo, B. Kuthanazhi, Y. Wu, R. J. McQueeney, A. Kaminski, and P. C. Canfield, Phys. Rev. B **99**, 245147 (2019).
[27] H.-Z. Lu and S.-Q. Shen, Front. Phys. **12**, 127201 (2017).
[28] K.-Y. Yang, Y.-M. Lu, and Y. Ran, Phys. Rev. B **84**, 075129 (2011).
[29] A. A. Burkov, Phys. Rev. Lett. **113**, 187202 (2014).
[30] A. A. Burkov, Phys. Rev. B **91**, 245157 (2015).
[31] S.-B. Zhang, H.-Z. Lu, and S.-Q. Shen, New J. Phys. **18**, 053039 (2016).
[32] See Sec. I of the Supplemental Material for detailed derivation of the scattering matrices in spin space.
[33] M. D. Stiles and A. Zangwill, Phys. Rev. B **66**, 014407 (2002).
[34] J. Zhang, P. M. Levy, S. Zhang, and V. Antropov, Phys.

Rev. Lett. **93**, 256602 (2004).

[35] S. S.-L. Zhang, G. Vignale, and S. Zhang, Phys. Rev. B **92**, 024412 (2015).

[36] S. S.-L. Zhang and G. Vignale, Phys. Rev. Lett. **116**, 136601 (2016).

[37] R. E. Camley and J. Barnaś, Phys. Rev. Lett. **63**, 664 (1989).

[38] See Sec. II of the Supplemental Material for detailed discussion of the Fermi arc surface states.

[39] See Sec. III of the Supplemental Material for a detailed discussion of the admissible evanescent surface states.

[40] L.-L. Wang, N. H. Jo, B. Kuthanazhi, Y. Wu, R. J. McQueeney, A. Kaminski, and P. C. Canfield, arXiv:1901.08234 .

[41] O. Mosendz, J. E. Pearson, F. Y. Fradin, G. E. W. Bauer, S. D. Bader, and A. Hoffmann, Phys. Rev. Lett. **104**, 046601 (2010).

[42] S. S.-L. Zhang, K. Chen, and S. Zhang, Europhys. Lett. **106**, 67007 (2014).

[43] A. A. Burkov, M. D. Hook, and L. Balents, Phys. Rev. B **84**, 235126 (2011).

[44] C. Fang, Y. Chen, H.-Y. Kee, and L. Fu, Phys. Rev. B **92**, 081201 (2015).

[45] E. Liu, Y. Sun, N. Kumar, L. Muechler, A. Sun, L. Jiao, S.-Y. Yang, D. Liu, A. Liang, Q. Xu, J. Kroder, V. Süß, H. Borrmann, C. Shekhar, Z. Wang, C. Xi, W. Wang, W. Schnelle, S. Wirth, Y. Chen, S. T. B. Goennenwein, and C. Felser, Nat. Phys. **14**, 1125 (2018).

[46] Q. Wang, Y. Xu, R. Lou, Z. Liu, M. Li, Y. Huang, D. Shen, H. Weng, S. Wang, and H. Lei, Nature Communications **9**, 3681 (2018).

[47] Y. Tserkovnyak, A. Brataas, G. E. W. Bauer, and B. I. Halperin, Rev. Mod. Phys. **77**, 1375 (2005).

[48] The spin current can be realized experimentally in a few different ways, for example through the SHE [6] or through spin pumping [47]; the manner through which the spin current is generated is not important for our purposes so we write the spin current in terms of an effective spin-dependent electric field.

[49] Note that in deriving Eq. (10) we have taken into account the fact that the equilibrium distribution of electrons in the WSM, i.e., $\hat{f}_{0,W}$, does not contribute to the current.